The end of the galactic cosmic-ray energy spectrum — a phenomenological view

Jörg R. Hörandel[1], **N.N.Kalmykov**[2], **A.V.Timokhin**[3]

[1] Institute for Experimental Nuclear Physics, University of Karlsruhe, P.O. Box 3640, 76021 Karlsruhe, Germany
[2] Skobeltsyn Institute of Nuclear Physics, Lomonosov Moscow State University, Russia
[3] Faculty of Physics, Lomonosov Moscow State University, Russia

E-mail: `hoerandel@ik.fzk.de`

Abstract. Two structures in the all-particle energy spectrum of cosmic rays, the knee at 4 PeV and the second knee around 400 PeV are proposed to be explained by a phenomenological model, the *poly-gonato* model, connecting direct and indirect measurements. Within this approach the knee is caused by a successive cut-off of the flux for individual elements starting with protons at 4.5 PeV. The second knee is interpreted as the end of the stable nuclei of the periodic table. To check some key features of this model calculations of the cosmic ray energy spectrum and the propagation path length at energies from 10^{14} to 10^{19} eV have been performed within the framework of a combined approach based on the diffusion model of cosmic rays and a direct simulation of charged-particle trajectories in the Galaxy.

1. Introduction

The all-particle energy spectrum of cosmic rays follows power laws over many orders of magnitude in energy. The flux decreases from values of several 1000 $(\mathrm{m}^2\ \mathrm{sr}\ \mathrm{s})^{-1}$ at GeV energies to values below 0.01 $(\mathrm{km}^2\ \mathrm{sr}\ \mathrm{a})^{-1}$ at energies exceeding 100 EeV. At a closer look some structures are seen in the spectrum. In particular, the *knee* around 4 PeV, the second *knee* at about 400 PeV, and the ankle above 4 EeV [1, 2]. In many contemporary models for galactic cosmic rays the *knee* is attributed to a cut-off for the flux of light elements at energies of several PeV, while the flux of heavier elements is supposed to continue to higher energies. As explanations the maximum energy attained during the acceleration process, diffusive losses from the Galaxy, or interactions close to the source, during propagation, as well as within the atmosphere are proposed [3].

The present work draws special attention on the second *knee* at energies around 400 PeV. The all-particle energy spectrum as obtained by several experiments is shown in Fig. 1 in the energy region around the second knee. A change of the steepening of the average all-particle spectrum around 400 PeV is visible. In the following the possibility is explored, that this structure can be interpreted as the end of the galactic cosmic-ray component. It should be pointed out that the position of the second *knee* is found to be at about $92 \times \hat{E}_p = 414$ PeV, where $\hat{E}_p = 4.5$ PeV is the position of the proton *knee* [2]. In such a picture all stable elements known from the periodic table of elements and found in cosmic rays are expected to contribute to the galactic cosmic-ray component. A cut-off for the individual elemental spectra for nuclei with charge number Z at energies $\hat{E}_Z = Z \cdot \hat{E}_p$ is anticipated.

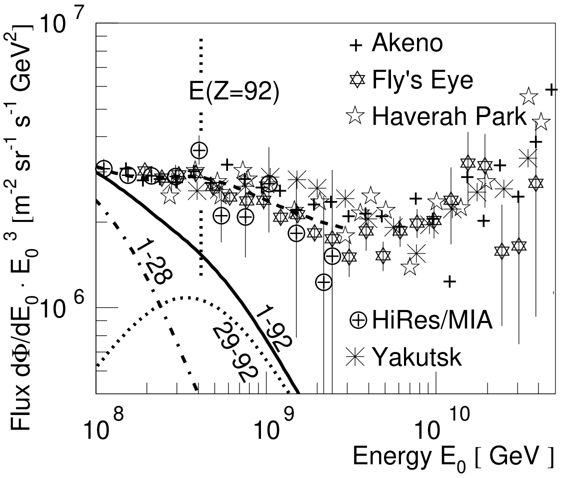

Figure 1. All-particle cosmic ray energy spectrum as obtained by several air shower experiments in the region of the second *knee*, for references see [2]. The lines indicate contributions for elemental groups with the given nuclear charge range. The cut-off energy $92 \cdot \hat{E}_p$ is indicated.

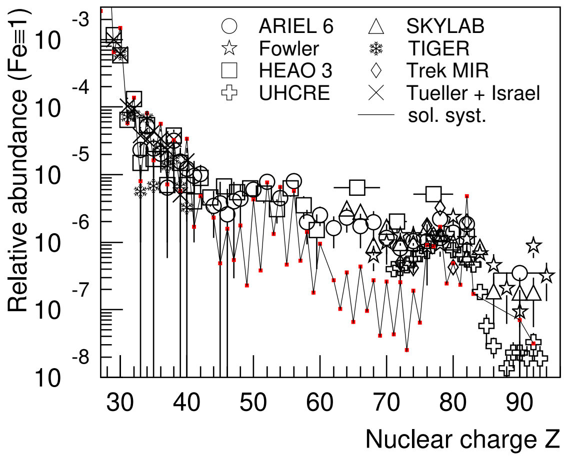

Figure 2. Relative abundance of cosmic-ray elements ($Z > 28$) normalized to Fe≡ 1 from various experiments around 1 GeV/n. For references see [2, 4]. For comparison, abundances in the solar system [5] are presented as well, normalized to Fe.

The sketched picture is based on the *poly-gonato* model. Its principle ideas are outlined in sect. 2. The model is a phenomenological approach connecting direct and indirect measurements of cosmic rays in the energy range from 1 GeV up to 1 EeV. The plausibility of some of its characteristic properties is checked by a detailed treatment of the propagation of cosmic rays in the Galaxy. In sect. 3 the propagation of cosmic-ray particles in the magnetic field of the Galaxy is investigated within a diffusion model. Predictions are discussed for the energy spectrum, the path length in the Galaxy, and the probability for a cosmic-ray particle to suffer nuclear interaction during propagation. A summarizing discussion (sect. 4) closes the article.

2. The Poly-Gonato Model

The basic idea of the *poly-gonato* model is to extrapolate the energy spectra as obtained by direct measurements to higher energies and compare the sum of all elements to the all-particle spectrum observed with air shower experiments [2]. Within the model the measured energy spectra of individual elements are parametrized assuming power laws and taking into account the solar modulation at low energies.

At energies in the GeV region the solar modulation of the energy spectra is described using the parametrization

$$\frac{d\Phi_Z}{dE}(E) = N\frac{E(E+2m_A)}{E+M} \cdot \frac{\left(E+M+780 \cdot e^{-2.5 \cdot 10^4 E}\right)^{\gamma_Z}}{E+M+2m_A}, \tag{1}$$

adopted from [6]. N is a normalization constant, γ_Z the spectral index of the anticipated power law at high energies (see below), $E = E_0/A$ the energy per nucleon, m_A the mass of the nucleus with mass number A, and M the solar modulation parameter. A value $M = 750$ MeV is used for the parametrization.

Above $Z \cdot 10$ GeV, the modulation due to the magnetic field of the heliosphere is negligible and the energy spectra of cosmic–ray nuclei are assumed to be described by power laws. However,

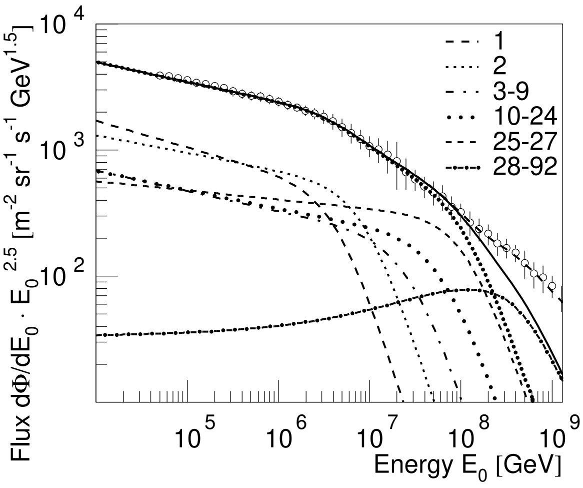

Figure 3. Cosmic ray energy spectra according to the *poly-gonato* model. The data points represent the normalized all-particle flux obtained by several experiments [2].

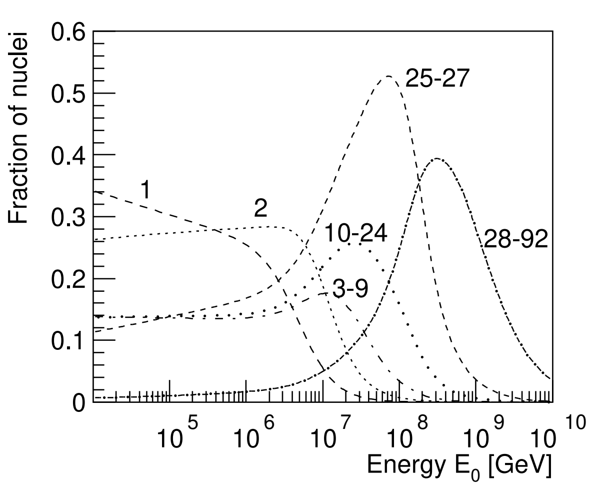

Figure 4. Relative fraction of elements with the indicated nuclear charge numbers according to the *poly-gonato* model.

extrapolating the elemental spectra with power laws, the all-particle spectrum obtained will overshoot the measured all-particle spectrum above several PeV. Hence, a cut-off in the spectra for the individual elements is introduced. Such a cut-off is motivated by various theories for the origin of the *knee* [3]. Inspired by such theories the following ansatz is adopted to describe the energy dependence of the flux for particles with charge Z

$$\frac{d\Phi_Z}{dE_0}(E_0) = \Phi_Z^0 E_0^{\gamma_Z} \left[1 + \left(\frac{E_0}{\hat{E}_Z}\right)^{\epsilon_c}\right]^{\frac{-\Delta\gamma}{\epsilon_c}} . \tag{2}$$

The absolute flux Φ_Z^0 and the spectral index γ_Z quantify the power law. The flux above the cut-off energy is modeled by a second and steeper power law. $\Delta\gamma$ and ϵ_c characterize the change in the spectrum at the cut-off energy $\hat{E}_Z$. Both parameters are assumed to be identical for all elements, $\Delta\gamma$ being the difference in the spectral indices below and above the respective *knees* and ϵ_c describes the smoothness of the transition from the first to the second power law. To study systematic effects also a common spectral index for all elements above their respective *knee* has been tried, see [2].

Different relations for the cut-off energy $\hat{E}_Z$ have been checked. The investigations showed that a rigidity dependent cut-off with $\hat{E}_Z = \hat{E}_p \cdot Z$, with the proton cut-off energy $\hat{E}_p$, fits the data best [2]. The all–particle spectrum is obtained by summation of the flux $d\Phi_Z/dE_0(E_0)$ for all cosmic–ray elements.

The absolute flux and the spectral indices for the elements from protons to nickel are derived from direct measurements above the atmosphere. For the heavier elements only abundances are known at energies around 1 GeV/n. In Fig. 2 the relative abundance normalized to Fe $\equiv 1$ is presented as function of the nuclear charge number. One recognizes that all elements up to the end of the periodic table are present. At energies of 1 GeV/n the measured abundances are heavily suppressed by the heliospheric modulation of cosmic rays — this is taken into account in the *poly-gonato* model using eq. (1). In addition, the measured abundances are extrapolated to high energies using an empirical relation for the spectral indices $-\gamma_Z = A + B \cdot Z^C$ with the values $A = 2.70 \pm 0.19$, $B = (-8.34 \pm 4.67) \cdot 10^{-4}$, and $C = 1.51 \pm 0.13$.

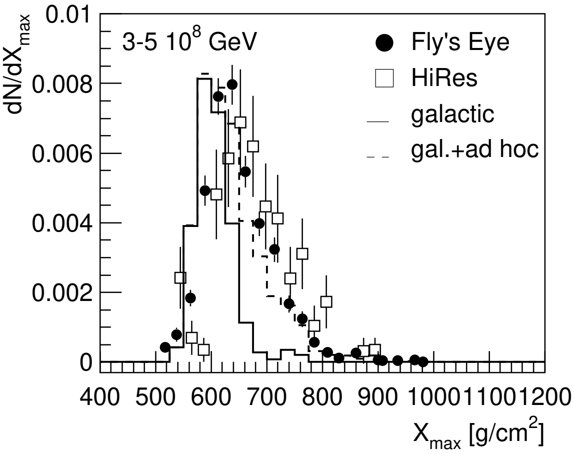

Figure 5. Distribution of the depth of the shower maximum X_{max} measured by the Fly's Eye [7] and HiRes [8] experiments. The measured values are compared with simulated results using QGSJET with lower cross sections [9]. Galactic component according to the *poly-gonato* model (solid line) and galactic plus *ad-hoc* component (dashed line), see also [9].

The average all-particle flux obtained by several air shower experiments is given in Fig. 3 by the data points. A fit to these points yields the parameters for the *poly-gonato* model $\hat{E}_p = 4.49 \pm 0.51$ PeV, $\Delta\gamma = 2.10 \pm 0.24$, and $\epsilon_c = 1.90 \pm 0.19$. The expected spectra for elemental groups corresponding to these parameters are shown in Fig. 3. The all-particle spectrum obtained by summation of all elements fits the experimental values well. It can be recognized that within this approach the *knee* is a consequence of the subsequential cut-offs for the individual elemental spectra, starting with protons at 4.5 PeV. The shape of the all-particle spectrum above this energy is determined by the overlay of the individual cut-offs for all elements. The second knee is related to the cut-offs for the heaviest elements at the end of the periodic table or the end of the galactic component.

The relative contributions of elemental groups to the all-particle spectrum are presented in Fig. 4. The most dominant group is the iron group ($Z = 25 - 27$), at energies around 70 PeV more than 50% of the all-particle flux consists of these elements. Ultra heavy elements ($Z \geq 28$) are expected to contribute at 300 PeV with slightly less than 40% to the all-particle flux.

Around 300 PeV measurements of the average depth of the shower maximum (X_{max}) are available from the Fly's Eye and HiRes experiments, see Fig. 5. These data are used to check the predictions of the *poly-gonato* model. With the air shower simulation program CORSIKA [10] and a modified version of the hadronic interaction model QGSJET with lower cross sections [9] the expected X_{max} distribution has been calculated. The composition of galactic cosmic rays has been assumed according to the *poly-gonato* model. The resulting distribution is given in Fig. 5 as solid histogram. It should be emphasized that this is not a fit to the measured X_{max} values, instead, the fluxes are taken as *predicted* by the model. As can be inferred from the figure, the left-hand side of the X_{max} distribution is represented quite reasonably. An *ad-hoc* component has been introduced to describe also the right-hand part of the distribution, for details see [9].

It should be pointed out that the three parameters of the model, namely $\hat{E}_p$, ϵ_c, and $\Delta\gamma$ in eq. (2) have been determined by a fit to the *all particle* spectrum derived from indirect measurements. That means the flux values for *individual elements* in the region of their cut-off are real predictions of the model. A comparison of the predicted fluxes with the energy spectra for groups of elements as recently derived from air shower measurements shows a quite satisfactory compatibility between the *poly-gonato* model and the measurements [3].

Two questions may rise when inspecting Fig. 3: Why are the spectra of heavy elements flatter than the spectra for light elements? And: can there be a sufficient contribution of ultra heavy elements at energies around 10^8 GeV? To obtain a quantitative estimate on this items in the following section the propagation of cosmic rays in the Galaxy is discussed.

3. Propagation of Cosmic Rays in the Galaxy

To study cosmic-ray propagation in the Galaxy, a detailed knowledge of the structure of the magnetic fields is essential. Unfortunately, the question about the configuration of the galactic magnetic field remains open — different models exist based on experimental data [11, 12, 13, 14]. How cosmic rays are accelerated to extremely high energies is another unanswered question. Although the popular model of cosmic-ray acceleration by shock waves in the expanding shells of supernovae (see e.g. [15, 16, 17]) is almost recognized as "standard theory," there are still a number of unresolved problems. Furthermore, the question about other acceleration mechanisms is not quite clear, and could lead to different cosmic-ray energy spectra at the sources [11].

Different concepts are verified by the calculation of the primary cosmic-ray energy spectrum, making assumptions on the density of cosmic-ray sources, the energy spectrum at the sources, and the configuration of the galactic magnetic fields. The diffusion model can be used in the energy range $E < 10^{17}$ eV, where the energy spectrum is calculated using the diffusion equation for the density of cosmic rays in the Galaxy. At higher energies this model ceases to be valid, and it becomes necessary to carry out numerical calculations of particle trajectories for the propagation in the magnetic fields of the Galaxy. This method works best for the highest energy particles, since the time for the calculations required is inversely proportional to the particle energy. Therefore, the calculation of the cosmic-ray spectrum in the energy range $10^{14} - 10^{19}$ eV has been performed within the framework of a combined approach, the use of a diffusion model and the numerical integration of particle trajectories.

3.1. Assumptions

High isotropy and a comparatively long retention of cosmic rays in the Galaxy ($\sim 10^7$ years for the disk model) reveal the diffusion nature of particle motion in the interstellar magnetic fields. This process is described by a corresponding diffusion tensor [11, 13, 18]. The steady-state diffusion equation for the cosmic-ray density $N(r)$ is (neglecting nuclear interactions and energy losses)

$$-\nabla_i D_{ij}(r) \nabla_j N(r) = Q(r). \tag{3}$$

$Q(r)$ is the cosmic-ray source term, $D_{ij}(r)$ is the diffusion tensor.

Under the assumption of azimuthal symmetry and taking into account the predominance of the toroidal component of the magnetic field, eq. (3) is presented in cylindrical coordinates as

$$\left[-\frac{1}{r}\frac{\partial}{\partial r} r D_\perp \frac{\partial}{\partial r} - \frac{\partial}{\partial z} D_\perp \frac{\partial}{\partial z} - \frac{\partial}{\partial z} D_A \frac{\partial}{\partial r} + \frac{1}{r}\frac{\partial}{\partial r} r D_A \frac{\partial}{\partial z} \right] N(r,z) = Q(r,z), \tag{4}$$

where $N(r,z)$ is the cosmic-ray density averaged over the large-scale fluctuations with a characteristic scale $L \sim 100$ pc [13]. $D_\perp \propto E^m$ is the diffusion coefficient, where m is much less than one ($m \approx 0.2$), and $D_A \propto E$ the Hall diffusion coefficient. The influence of Hall diffusion becomes predominant at sufficiently high energies ($> 10^{15}$ eV). The sharp enhancement of the diffusion coefficient leads to the excessive cosmic-ray leakage from the Galaxy at energies $E > 10^{17}$ eV. For investigating the cosmic-ray propagation at such energies it is necessary to carry out calculations of the trajectories for individual particles.

The numerical calculation of trajectories is based on the solution of the equation of motion for a charged particle in the magnetic field of the Galaxy. The calculation was carried out using a fourth order Runge-Kutta method. Trajectories of cosmic rays were calculated until they left the Galaxy. Testing the differential scheme used, it was found that the accuracy of the obtained trajectories for protons with an energy $E = 10^{15}$ eV after passing a distance of 1 pc amounts to $5 \cdot 10^{-8}$ pc. The retention time of a proton with such an energy averages to about 10 million

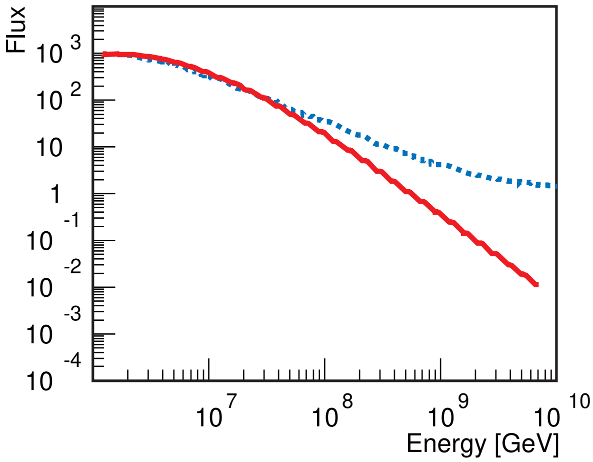

Figure 6. Calculated spectra for protons for the diffusion model (solid line) and the numerical trajectory calculations (dotted line).

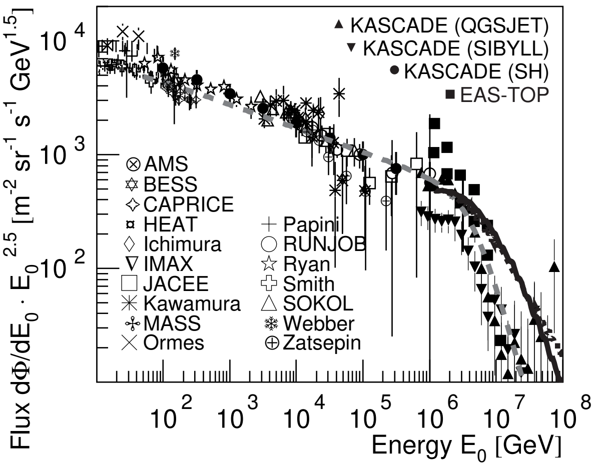

Figure 7. Proton flux as obtained from various measurements, for references see [21], compared to the spectra shown in Fig. 6 and the *poly-gonato* model (dashed line).

years, hence, a total error for the trajectory approximation by the differential scheme is about 0.5 pc.

The magnetic field of the Galaxy consists of a large-scale regular and a chaotic component $\vec{B} = \vec{B}_{reg} + \vec{B}_{irr}$. A purely azimuthal magnetic field was assumed for the regular field

$$B_z = 0, \quad B_r = 0, \quad B_\phi = 1\ \mu\text{G} \cdot \exp\left(-\frac{z^2}{z_0^2} - \frac{r^2}{r_0^2}\right), \tag{5}$$

where $z_0 = 5$ kpc and $r_0 = 10$ kpc are constants [13]. The irregular field was constructed according to an algorithm used in [19], that takes into account the correlation of the magnetic field intensities in adjacent cells. The radius of the Galaxy is assumed to be 15 kpc and the galactic disk has a half-thickness of 200 pc. The position of the Solar system was defined at $r = 8.5$ kpc, $\phi = 0°$, and $z = 0$ kpc. A radial distribution of supernovae remnants along the galactic disk was considered as sources [20].

3.2. Results

The results for the calculations of the cosmic-ray proton spectrum are presented in Fig. 6. These results were obtained using the diffusion model and numerical calculations of trajectories. It is evident from the graph that both methods give identical results up to about $3 \cdot 10^7$ GeV. At higher energies there is a continuous decrease of the intensity in the diffusion spectrum, which corresponds to the excessive increase in the diffusion coefficient that leads to a large leakage of particles from the Galaxy.

An energy of 10^{17} eV can be defined as the conventional boundary to apply the diffusion model. At this energy the results obtained with the two methods differ by a factor of two and for higher energies the diffusion approximation becomes invalid.

The predicted spectra are compared to direct and indirect measurements of the primary proton flux in Fig. 7. In the depicted range there is almost no difference between the two approaches. The relatively steep decrease of the flux at energies exceeding 4 PeV is not reflected. On the other hand, the data are described reasonably well by the *poly-gonato* model, as also shown in the figure. The observed change in the spectral index $\Delta\gamma \approx 2.1$ according to the

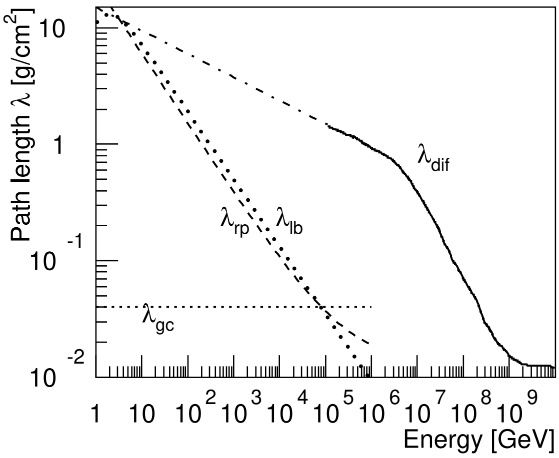

Figure 8. Path length in the Galaxy for protons. The values for the diffusion model (λ_{dif}) are indicated by the solid line. They are extrapolated to lower energies by the dashed dotted line. The dashed and dotted lines indicate a leaky-box model (λ_{lb}, eq. (6)) and a residual path length model (λ_{rp}, eq. (7)). The dotted line indicates the matter accumulated along a straight line from the galactic center to the solar system (λ_{gc}).

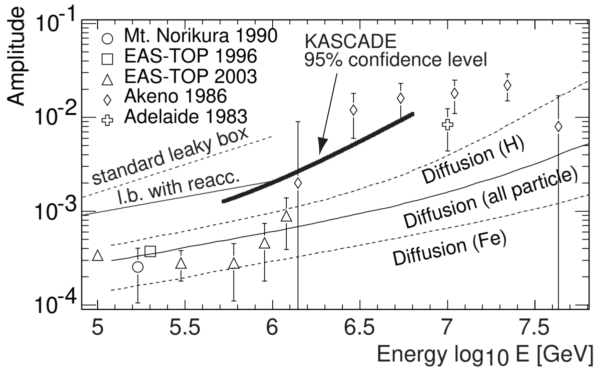

Figure 9. Rayleigh amplitudes as function of energy for various experiments, for references see [22]. Additionally, model predictions for leaky-box models [23] and a diffusion model [24] are shown. The lines indicate the expected anisotropy for primary protons, iron nuclei, and all particles.

poly-gonato model has to be compared to the value predicted by the diffusion model. In the latter the change should be $1 - m \approx 0.8$ [13]. The observed value is obviously larger, which implies that the remaining change of the spectral shape should be caused by a change of the spectrum at the source, e.g. due to the maximum energy attained in the acceleration process.

The maximum energy and, therefore, the energy at which the spectrum steepens depends on the intensity of the magnetic fields in the acceleration zone and on a number of assumptions for the feedback of cosmic rays to the shock front. The uncertainty of the parameters yields variations in the maximum energy predicted by different models up to a factor of 100 [3, 16]. Thus, there is no consensus about what the "standard model" is considered to predict. For the time being, it is difficult to make definite conclusions from the comparison between the experimental spectra for different elemental groups and the "standard model" of cosmic ray acceleration at ultra high energies.

The obtained path length (λ_{dif}) in the Galaxy for protons as function of energy is presented in Fig. 8. The interstellar matter density was taken as $n_d = 1$ cm^{-3} for the galactic disk and $n_h = 0.01$ cm^{-3} for the halo. For heavier nuclei with charge Z the path length scales with the rigidity, i.e. is related to the values for protons $\lambda(E)$ as $\lambda(E, Z) = \lambda(E/Z)$. At the corresponding knees, the amount of traversed material is less than 1 g/cm^2. The dashed dotted line indicates a trend at lower energies according to $\lambda \propto E^{-\delta}$. To reach values around 10 g/cm^2 as obtained around 1 GeV, see below, one needs a relatively small slope $\delta \approx 0.2$ — much lower than the value usually assumed $\delta \approx 0.6$.

Measurements of the ratio of secondary to primary cosmic-ray nuclei at GeV energies are successfully described using a leaky-box model. For example, assuming the escape path length

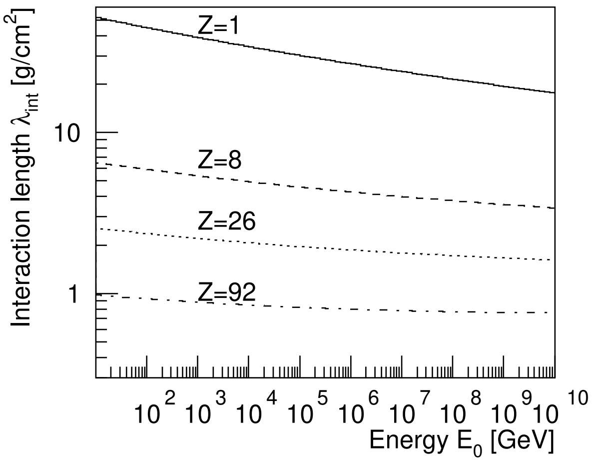

Figure 10. Interaction length for different elements based on cross-sections according to the hadronic interaction model QGSJET, the respective nuclear charge number is indicated.

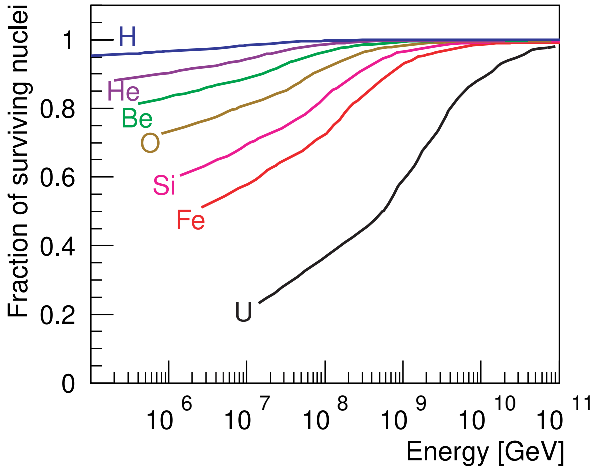

Figure 11. Fraction of nuclei surviving without interaction in the Galaxy for different elements.

as

$$\lambda_{lb} = \frac{26.7\beta \text{ g/cm}^2}{(\beta R/1.0 \text{ GV})^{0.58} + (\beta R/1.4 \text{ GV})^{-1.4}} \tag{6}$$

various secondary to primary ratios obtained by the ACE/CRIS and HEAO-3 experiments can be described consistently in the energy range from ~ 70 MeV to ~ 30 GeV [25]. A similar approach is the residual path length model [26], assuming the relation

$$\lambda_{rp} = \left[6.0 \cdot \left(\frac{R}{10 \text{ GV}}\right)^{-0.6} + 0.013\right] \text{ g/cm}^2 \tag{7}$$

for the escape path length. Both examples are compared to the predictions of the diffusion model in Fig. 8.

Extrapolating these relations to higher energies, the strong dependence of the path length on energy ($\propto E^{-0.6}$) leads to extremely small values at PeV energies. Above 10^5 GeV the traversed matter would be less than the matter accumulated along a straight line from the galactic center to the solar system $\lambda_{gc} = 8 \text{ kpc} \cdot 1 \text{ proton/cm}^3 \approx 0.04 \text{ g/cm}^2$. This value is indicated in Fig. 8 as dotted line.

A similar conclusion can be derived from anisotropy measurements. Rayleigh amplitudes observed by different experiments are compiled in Fig. 9 [22]. Leaky-box models, with their extremely steep decrease of the path length $\lambda \propto E^{-0.6}$, yield relative large anisotropies even at modest energies, which seem to be ruled out by the measurements. Two versions of a leaky-box model [23], with and without reacceleration are represented in the figure. On the other hand, a diffusion model [24], which is based on the same basic idea [13] as the present work, seems to be compatible with the measured data. For this model the expected Rayleigh amplitudes are given for primary protons and iron nuclei, as well as for a mixture of all elements.

Using nuclear cross sections according to the hadronic interaction model QGSJET [27] and assuming a number density $n_p = 1$ proton/cm^3 in the galactic disk, the interaction length of nuclei has been calculated. The results for four different elements are presented in Fig. 10. The values decrease slightly as function of energy. Values for protons are in the range $20 - 55$ g/cm^2, the values decrease as function of nuclear charge and reach values < 1 g/cm^2 for the heaviest elements.

The interaction probability for different nuclei has been calculated based on the obtained path length and interaction parameters according to the QGSJET model. Nuclear fragmentation is taken into account in an approximate approach [28]. It should be pointed out that a nuclear fragment conserves the trajectory direction of its parent if Z/A in question is the same as for the primary nucleus and for most stable nuclei the ratio Z/A is close to 1/2. The resulting fraction of nuclei which survive without an interaction is presented in Fig. 11 for selected elements. It turns out that at the respective knees ($Z \cdot 4.5$ PeV) more than about 50% of the nuclei survive without interactions, even for the heaviest elements. This is an important result, since the *poly-gonato* model relates the contribution of ultra-heavy cosmic rays to the second knee in the all-particle spectrum around 400 PeV. It should be noted that the fraction of surviving nuclei would be even larger for a leaky-box model, with its low path length at such energies.

4. Discussion

The energy spectrum of cosmic rays at their source $Q(E)$ is related to the observed values at Earth $N(E)$ as

$$N(E) = Q(E) \left(\frac{1}{\lambda_{esc}(E)} + \frac{1}{\lambda_{int}(E)} \right)^{-1} \tag{8}$$

with the propagation path length λ_{esc} and the interaction length λ_{int}. The corresponding values are presented in Fig. 8 and Fig. 10, respectively. It is frequently assumed that the propagation path length decreases as function of energy $\lambda_{lb} \propto E^{-0.6}$, as discussed above. Since the interaction length is almost independent of the primary energy this necessitates a spectrum at the sources $Q(E) \propto E^{-2.1}$ to explain the observed spectrum at Earth $N(E) \propto E^{-2.7}$. However, the model by Berezhko *et al* [16] predicts even flatter spectra at the sources before the *knee* and an even stronger dependence of λ_{esc} on energy is needed. Recent measurements of the TeV γ ray flux from a shell type supernova remnant yield a spectral index $\gamma = -2.19 \pm 0.09 \pm 0.15$ [29] in agreement with the "standard model". However, e.g. for the Crab Nebula a steeper spectrum with $\gamma = -2.57 \pm 0.05$ has been obtained [30], indicating that not all sources exhibit the same behaviour.

As has been discussed above, the dependence of the propagation path length $\lambda_{esc} \propto E^{-0.6}$ can not be extrapolated to *knee* energies. Taking a value $\lambda_{esc} \propto E^{-0.2}$ as discussed in relation with Fig. 8 necessitates additional assumptions on the spectral shape $Q(E)$ at the source in order to explain the observed spectra with spectral indices in the range $-\gamma \approx 2.55 - 2.75$ [2].

Direct measurements seem to indicate that the spectra of light elements are flatter as compared to heavy elements [2]. The values of λ_{int} for protons are at all energies larger than the escape path length λ_{dif}. Hence, for protons the escape from the Galaxy is the dominant process influencing the shape of the observed energy spectrum. For iron nuclei at low energies hadronic interactions are dominating ($\lambda_{int} \approx 2$ g/cm$^2 < \lambda_{dif}$) and leakage from the Galaxy becomes important at energies approaching the iron knee ($26 \times \hat{E}_p$). However, for elements heavier than iron the interaction path length is smaller than the escape path length for all energies, except above the respective *knees*. At low energies the propagation path length exceeds the interaction path length by about an order of magnitude. For these elements nuclear interaction processes are dominant for the shape of the observed spectrum. This may explain why energy spectra for heavy elements should be flatter as compared to light nuclei. In particular, the ultra-heavy elements suffer significantly from interactions at low energies.

In **summary**, the results obtained show the effectiveness of the combined method to calculate the cosmic-ray spectrum using a numerical calculation of trajectories and a diffusion approximation. The calculated dependence of the propagation path length on energy suggests that the difference between the predicted spectral index at the source ($\gamma \approx -2.1$) in the "standard model" and the experimental value ($\gamma \approx -2.7$) can not be explained by the energy dependence of the escape path length solely. The compatibility of the observed cosmic-ray energy spectrum with the "standard model" requires additional assumptions. Most likely, it can be concluded that the *knee* in the energy spectrum of cosmic rays has its origin in both, acceleration and propagation processes.

In the *poly-gonato* model the *knee* in the energy spectrum at 4.5 PeV is caused by a cut-off of the light elements and the spectrum above the *knee* is determined by the subsequent cut-offs of all heavier elements at energies proportional to their nuclear charge number. The second *knee* around 400 PeV $\approx 92 \cdot \hat{E}_p$ is due to the cut-off of the heaviest elements in galactic cosmic rays. Considering the calculated escape path length and nuclear interaction length within the diffusion model, it seems to be reasonable that the spectra for heavy elements are flatter as compared to light elements. The calculations show also that even for the heaviest elements at the respective *knee* energies more than 50% of the nuclei survive the propagation process without interactions. This may explain why ultra-heavy elements are expected to contribute significantly ($\sim 40\%$) to the all-particle flux at energies around 400 PeV.

Acknowledgements
The authors are grateful to J. Engler, A.I. Pavlov, and V.N. Zirakashvili for useful discussions. N.N.K. and A.V.T. acknowledge the support of the RFBR (grant 05-02-16401).

References

[1] M. Nagano & A.A. Watson, *Rev. Mod. Phys.* **72**, 689 (2000).
[2] J.R. Hörandel, *Astropart. Phys.* **19**, 193 (2003).
[3] J.R. Hörandel, *Astropart. Phys.* **21**, 241 (2004).
[4] J.T. Link *et al.*, *Proc. 28th Int. Cosmic Ray Conf., Tsukuba* **4**, 1781 (2003).
[5] A.G.W. Cameron, *Space Sci. Rev.* **15**, 121 (1973).
[6] G. Bonino *et al.*, *Proc. 27th Int. Cosmic Ray Conf., Hamburg* **9**, 3769 (2001).
[7] T.K. Gaisser *et al.*, *Phys. Rev. D* **47**, 1919 (1993).
[8] T. Abu-Zayyad *et al.*, *Astrophys. J.* **557**, 686 (2000).
[9] J.R. Hörandel, *J. Phys. G: Nucl. Part. Phys.* **29**, 2439 (2002).
[10] D. Heck *et al.*, Report FZKA 6019, Forschungszentrum Karlsruhe (1998).
[11] V.S. Berezinsky *et al.*, *Astrophysics of Cosmic Rays*, North-Holland (1990).
[12] A.A. Ruzmaikin *et al.*, *Magnetic Fields of Galaxies*, Kluwer, Dordrecht (1988).
[13] S.V. Ptuskin *et al.*, *Astron. & Astroph.* **268**, 726 (1993).
[14] E.V. Gorchakov & I.V. Kharchenko, *Izv. RAN ser. phys.* **64**, 1457 (2000).
[15] D.C. Ellison *et al.*, *Astrophys. J.* **488**, 197 (1997).
[16] E.G. Berezhko & L.T. Ksenofontov, *JETP* **89**, 391 (1999).
[17] L.G. Sveshnikova *et al.*, *Astron. & Astroph.* **409**, 799 (2003).
[18] N.N. Kalmykov & A.I. Pavlov, *Proc. 26th Int. Cosmic Ray Conf., Salt Lake City* **4**, 263 (1999).
[19] V.N. Zirakashvili *et al.*, *Izv. RAN ser. phys.* **59**, 153 (1995).
[20] K. Kodaira, *Publ. Astron. Soc. Japan* **26**, 255 (1974).
[21] J.R. Hörandel, *astro-ph/0407554* (2004).
[22] T. Antoni *et al.*, *Astrophys. J.* **604**, 687 (2004).
[23] V.S. Ptuskin, *Adv. Space Res.* **19**, 697 (1997).
[24] J. Candia *et al.*, *J. Cosmol. Astropart. Phys.* **5**, 3 (2003).
[25] N.E. Yanasak *et al.*, *Astrophys. J.* **563**, 768 (2001).
[26] S.P. Swordy, *Proc. 24th Int. Cosmic Ray Conf., Rome* **2**, 697 (1995).
[27] N.N. Kalmykov *et al.*, *Nucl. Phys. B (Proc. Suppl.)* **52B**, 17 (1997).
[28] N.N. Kalmykov & S.S. Ostapchenko, *Yad. Fiz.* **56**, 105 (1993).
[29] F. Aharonian *et al.*, *Nature* **432**, 75 (2004).
[30] C. Masterson *et al.*, *2nd Int. Symp. on High Energy Gamma Ray Astronomy, Heidelberg, 2004, APS Conf. Proc. 745* p. 617 (2004).